CrossMark

ORIGINAL PAPER

Preparation, characterization and catalytic activity of dendrimer-encapsulated phosphotungstic acid nanoparticles immobilized on nanosilica for the synthesis of 2*H*-indazolo[2,1-*b*] phthalazine-triones under solvent-free or sonochemical conditions

Mohsen Esmaeilpour[1] · Jaber Javidi[2,3] · Farzaneh Dehghani[1]

Abstract   In this paper, we adopt a facile method to prepare a type of porous silica nanoparticles (n-SiO$_2$) from tetraethyl orthosilicate as the source of silica. Then, dendritic polymer supported on nanosilica with surface amino groups was fabricated. Finally, H$_3$PW$_{12}$O$_{40}$ nanoparticles (PWA^n) were synthesized by the treatment of H$_3$PW$_{12}$O$_{40}$ powder with n-Octane as solvent by a solvothermal method and then immobilized onto the dendrimer polymer functionalized nanosilica. The synthesized nanostructures were characterized by fourier transform infrared (FT-IR), X-ray diffraction (XRD), thermogravimetric analysis (TGA), dynamic light scattering (DLS), N$_2$ adsorption–desorption isotherm analysis, UV–Vis and elemental analysis. The morphology of the catalyst was characterized using transmission electron microscopes (TEM). The acidity of the catalyst was determined by FTIR pyridine adsorption spectroscopy. Then, this catalytic system was used as an efficient catalyst for the synthesis of 2H-indazolo[2,1-b]phthalazine-triones via multi-component and one-pot reactions of various aldehydes, phthalic anhydride, hydrazinium hydroxide, and dimedone under thermal solvent-free conditions or ultrasound irradiation at room temperature. Also, the catalyst can be easily recovered and reused for six consecutive reaction cycles without significant loss of activity.

✉ Mohsen Esmaeilpour
  m1250m551085@yahoo.com

✉ Jaber Javidi
  jaberjavidi@gmail.com; jaberjavidi@sbmu.ac.ir

1   Chemistry Department, College of Science, Shiraz University, 71454 Shiraz, Iran

2   Department of Pharmaceutics, School of Pharmacy, Shahid Beheshti University of Medical Sciences, Tehran, Iran

3   Students Research Committee, School of Pharmacy, Shahid Beheshti University of Medical Sciences, Tehran, Iran

Introduction

The development of simple synthetic routes for complex organic molecules from readily available reagents is an important task in organic synthesis. Multicomponent (MCRs) protocol emphasizes as one-pot reaction in which three or more reactants are combined together to generate a single product with greater efficiency [1]. Multicomponent reactions enable multiple reactions leading to interesting heterocyclic scaffolds which are useful for the construction of poly-functionalized heterocyclic 'drug like' libraries [2].

Nitrogen-containing heterocyclic compounds are well known in nature, and their applications to pharmaceuticals, agrochemicals, and functional materials are becoming more and more important [3]. Among a large variety of heterocyclic compounds, bridgehead nitrogen heterocycles containing a phthalazine moiety are of interest because they exhibit pharmacological and biological activities including, antimicrobial [4] and anticonvulsant [5]. Nevertheless, the development of new synthetic methods for the efficient preparation of heterocycles containing phthalazine ring fragment is an interesting challenge. A number of methods have been reported for the synthesis of phthalazine derivatives such as three-component condensation of phthalhydrazide, dimedone, and aromatic aldehydes [6–8] or four-component reaction of phthalic anhydride, hydrazinium hydroxide, dimedone and aromatic aldehydes in the presence of various catalysts such as heteropoly acids (HPAs) [9], ZnO nanoparticles [10] and etc.

🙂 Springer

Heteropolyacids (HPAs) have been used as efficient catalysts for a variety of organic reactions [11–17]. Although HPAs in their acidic form are versatile compounds, their main disadvantages are high solubility in polar solvents and low surface area. In previous study [18] we find that by reducing the particle size of PWA from bulk powder to nanometer scale, the surface area increased from 12 to 242 m^2/g. Furthermore, acidity and catalytic activity of HPAs rising by declining particle size or increasing of surface area [19]. The use of support is another approach, that allows the heteropolyacids to be dispersed over a large surface area and increases theirs catalytic activity. Silica is a very important industrial material and is extensively used for a wide range of commercial applications such as catalyst supports, molecular sieves, resins, fillers in polymers, as well as in biomedical applications [20]. In particular, silica nanoparticles with high surface area are of high interest to many key chemical applications [21].

Dendrimers are a well-recognized class of precise macromolecules that should find multiple applications in molecular electronics [22], catalysis [23] and biomedical applications [24, 26, 27].

The use of ultrasonic irradiation accelerates an organic transformation at ambient conditions which otherwise require harsh conditions of temperature and pressure [28]. The interaction between molecules and ultrasound is not direct but the energy of theses long wavelength can cause cavitation which makes the reaction faster [29].

Therefore, as part of our continuing interest in developing of recyclable nanocatalyst in synthesis of useful compounds [30], we report on the preparation of dendrimer-encapsulated phosphotungstic acid nanoparticles immobilized on nanosilica (Dendrimer-PWA^n) as recyclable catalyst (Scheme 1) for the one-pot synthesis of 2H-indazolo [2,1-b] phthalazine-triones via a one-pot four-component reaction from simple and easily available starting materials under much milder reaction conditions.

Experimental

General

Chemicals were purchased from Merck and Aldrich Chemical Companies. All other chemicals are analytical grade and used without further purification. Fourier transform infrared spectroscopy (FT-IR) analysis of the samples was taken on a Shimadzu FT-IR 8300 spectrophotometer and the sample and KBr were pressed to form a tablet. The NMR spectra were recorded on a Bruker avance DPX 500 MHz spectrometer in chloroform (CDCl$_3$) using tetramethylsilane (TMS) as an internal reference. X-ray powder diffraction (XRD) analysis was conducted on a Bruker AXS D8-advance

X-ray diffractometer using Cu Kα radiation ($\lambda = 1.5418$). Transmission electron microscopy (Philips EM208) with an accelerating voltage of 100 kV was used to examine morphology and size of the nanoparticles and dynamic light scattering (DLS) was recorded on a HORIBA-LB550. The n-SiO$_2$ and Dendrimer-PWA^n were dispersed on ethanol solution under ultrasonic vibration for 10 min and one drop of the suspension evaporated onto a carbon-coated copper grid for TEM measurement. TGA thermograms were recorded on an instrument of Perkin Elmer with N$_2$ carrier gas and the rate of temperature change of 20 °C min^{-1}. BET surface area and porosity of catalysts were determined from nitrogen adsorption isotherm by the Brunauer-Emmett-Teller (BET) method and determination of the pore size distribution from adsorption branch by the Barrett-Joyner-Halenda (BJH) method. Diffuse reflectance UV–visible measurements were recorded at room temperature on a Perkin-Elmer Lambda 650 spectrometer. Tungsten contents in the Dendrimer-PWA^n sample were estimated by inductively coupled plasma-atomic emission spectroscopy (ICP-AES). The C, H, N and S elemental analyses were carried out by the using a Thermofinigan Flash EA-1112 CHNSO rapid elemental analyzer. Melting points were determined with a Buchi 510 instrument in open capillary tubes and are uncorrected. Determination of the purity of the substrate and monitoring of the reaction were accomplished by thinlayer chromatography (TLC) on a silica gel polygram SILG/UV 254 plates. Therefore, all of the products were characterized by FT-IR, ^{1}H NMR and ^{13}C NMR, and also by comparison with authentic samples.

## Synthesis of dendrimer-encapsulated phosphotungstic acid nanoparticles immobilized on nanosilica

Synthesis of silica nanoparticles

0.5 ml TEOS was added into the mixture of 50 ml ethanol, 20 ml water and 0.5 ml ethylenediamine under ultrasonic irradiation [25]. After 30 min, the precipitate was isolated by centrifuging and washed with ethanol and water several times. The as-obtained products were dried at 80 °C under vacuum for 2 h and then were calcined at 650 °C for 2 h.

Preparation of functionalized SiO$_2$ nanoparticle with 3-chloro triethoxy propyl silane (nSiO$_2$-Cl)

Nano SiO$_2$ (1 g) was added to the solution of 3-chloro triethoxy propylsilane (10 mmol, 2.4 mL) in ethanol (10 mL) and the resultant mixture was under reflux for 10 h under nitrogen atmosphere [27]. After refluxing, the mixture was cooled to room temperature and the solid product was filtered off, washed with ethanol and water to remove unreacted species and dried at 60 °C for 8 h.

Scheme 1 Process for preparation of nanosilica supported dendritic polymer
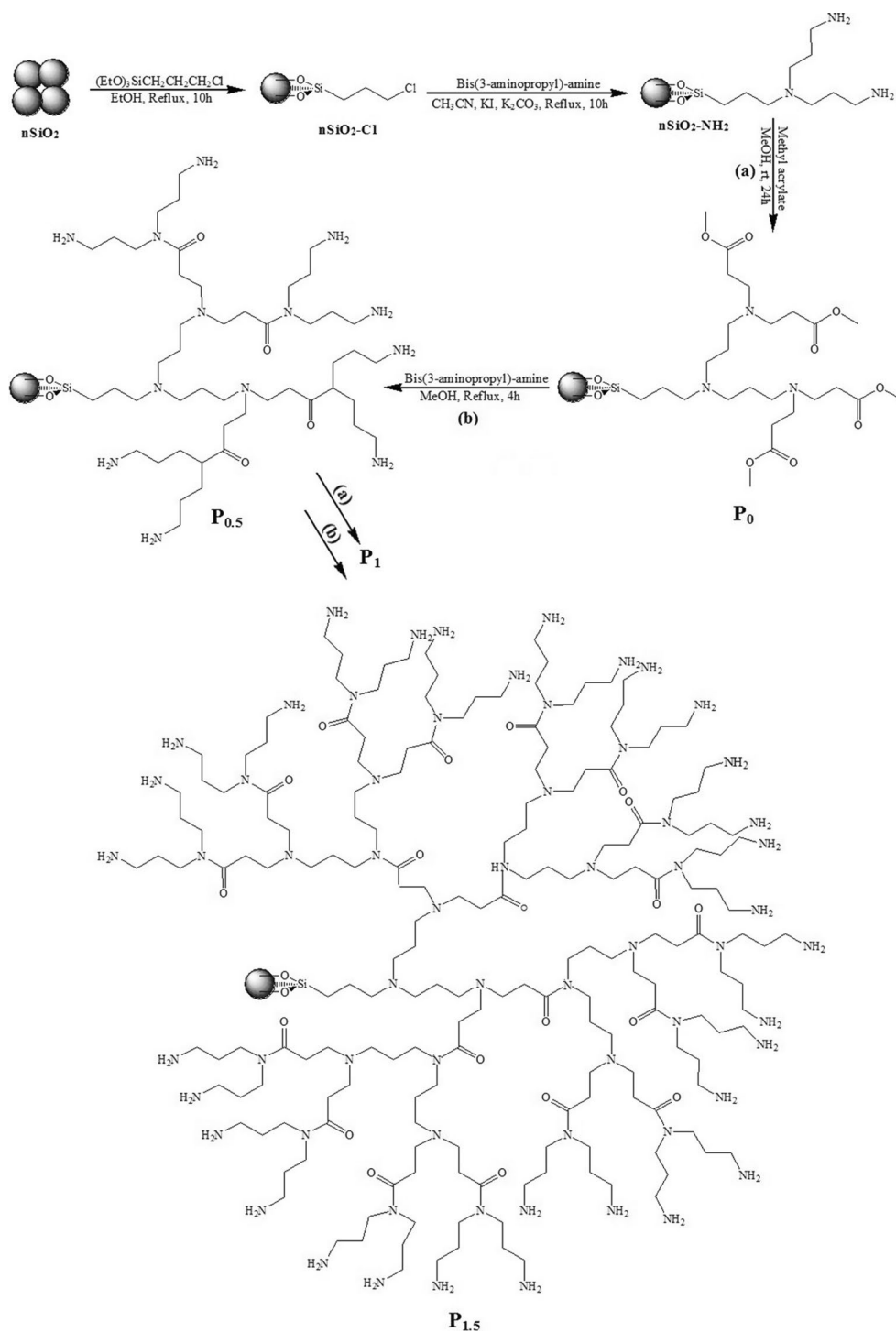
Preparation of nSiO₂-NH₂

In a typical synthetic procedure [30], 1.2 mL (10 mmol) of bis(3-aminopropyl) amine was added to a suspension of nSiO₂-Cl (1.0 g) in 10 mL acetonitrile, potassium iodide (10 mmol, 1.66 g) and potassium carbonate (10 mmol, 1.38 g). The reaction mixture was refluxed in an oil bath for 10 h. The solid product was filtered off, washed with

sufficient amount of distilled water, and dried at 60 °C for 12 h to afford nSiO₂-NH₂ nanoparticles.

Preparation of P₀

nSiO₂-NH₂ (1 g) was added to the stirred solution of methyl acrylate (20 mmol, 1.7 mL) in methanol (10 mL). The final mixture was stirred at room temperature for 24 h.

Then, the solid material was separated by filtration, washed with hot methanol for 6 h in a Soxhlet apparatus to remove the unreacted starting materials and then finally dried in a vacuum oven at 60 °C.

Preparation of nanosilica supported dendritic polymer ($P_{0.5}$)

To a slurry of P_0 (1 g) in methanol (10 mL) was added bis(3-aminopropyl) amine (20 mmol, 2.4 mL). The reaction mixture was refluxed with continuous stirring under inert atmosphere for 4 h. Final product was filtered, washed with hot methanol for 6 h in a Soxhlet apparatus to remove the unreacted starting materials and then dried in a vacuum oven at 60 °C [23].

Preparation of nanosilica supported dendritic polymer ($P_{1.5}$)

A well stirred solution of methyl acrylate (40 mmol, 3.4 mL) in methanol (15 ml) was added to the stirred solution of $P_{0.5}$ (1 g). The final mixture was stirred at room temperature for 24 h. Then, the solid material (P_1) was separated by filtration, washed with hot methanol for 6 h in a Soxhlet apparatus to remove the unreacted starting materials and then finally dried in a vacuum oven at 60 °C. Then, bis(3-aminopropyl) amine (40 mmol, 4.8 mL) was added to a stirred solution of P_1 (1 g) in 15 mL methanol. The final mixture was refluxed with continuous stirring under inert atmosphere for 6 h Final product ($P_{1.5}$) was filtered, washed with hot methanol for 6 h in a Soxhlet apparatus to remove the unreacted starting materials and then dried in a vacuum oven at 60 °C [23].

Synthesis of $H_3PW_{12}O_{40}$ nanoparticles (PWA^n)

PWA^n nanoparticles were prepared in our previous work [18]. $H_3PW_{12}O_{40}$ nanoparticles (which were labeled as PWA^n) were composed by heat treatment of their bulky forms in an autoclave. HPAs are soluble in polar solvents such as methanol and water but are insoluble in non-polar solvent such as hexane. In a typical procedure, 0.3 mmol of bulk $H_3PW_{12}O_{40}.14H_2O$ (PWA^b) was dispersed in 50 ml hexane and the obtained mixture was stirred vigorously for 30 min at room temperature in order to forming a homogeneous dispersion. This dispersion was transferred into a Teflon-lined stainless autoclave and filled 80 % of its total volume. The autoclave was sealed and maintained at 150 °C for 12 h and then was cooled to room temperature. Finally, the produced powder was filtered and dried in a vacuum at 60 °C for 12 h.

Preparation of dendrimer-encapsulated phosphotungstic acid nanoparticles immobilized on nanosilica (Dendrimer-PWA^n)

For the anchoring of PWA^n on to $P_{1.5}$. 2 g of $P_{1.5}$ was dispersed in 40 mL of n-Hexane and ultrasonicated for 30 min. Then, PWA^n (0.5 mmol, 1.48 g) was added into the solution and ultrasonicated for 30 min and the mixture was stirred for 24 h at room temperature. Finally, the formed Dendrimer-PWA^n was washed with distilled water for several times and then dried in a desiccator for 6 h. The sample thus prepared was designated as Dendrimer-PWA^n and stored in airtight bottle for further use.

General procedure for the synthesis of 2H-indazolo[2,1-b] phthalazine-triones under solvent-free conditions

A mixture of dimedone (1 mmol), aldehyde (1 mmol), hydrazinium hydroxide (1.2 mmol), phthalic anhydride (1 mmol) and Dendrimer-PWA^n catalyst (0.01 g, 0.14 mol %) was heated at 80 °C for the time indicated in Table 2. The reactions were followed by thin layer chromatography (TLC) using hexane/ethyl acetate (3:1) as an eluent. After completion of the reaction as indicated by TLC, the reaction mixture was cooled, the solid residue was dissolved in hot EtOH and the catalyst was filtered off. The filtrate solution was evaporated under vacuum, and the solid crude product was purified by recrystallized from ethanol for more purification.

General procedure for the synthesis of 2H-indazolo[2,1-b]phthalazine-triones by ultrasound irradiation

Dimedone (1 mmol), aldehyde (1 mmol), hydrazinium hydroxide (1.2 mmol) and phthalic anhydride (1 mmol) were added to Dendrimer-PWA^n catalyst (0.015 g, 0.21 mol %) in a 25 mL Pyrex flask. The mixture was continuously irradiated for the appropriate time (Table 2) at room temperature (solid paste using a drop of acetonitrile was prepared in case of solid aldehydes). The reactions were followed by thin layer chromatography (TLC) using hexane/ethyl acetate (3:1). The temperature was controlled and fixed at room temperature by pouring cold water in the bath in the case of any elevation of temperature. After completion of the reaction as indicated by TLC, the solid residue was dissolved in hot EtOH and the catalyst was filtered off. The filtrate solution was evaporated under vacuum, and the solid crude product was purified by recrystallized from ethanol for more purification.
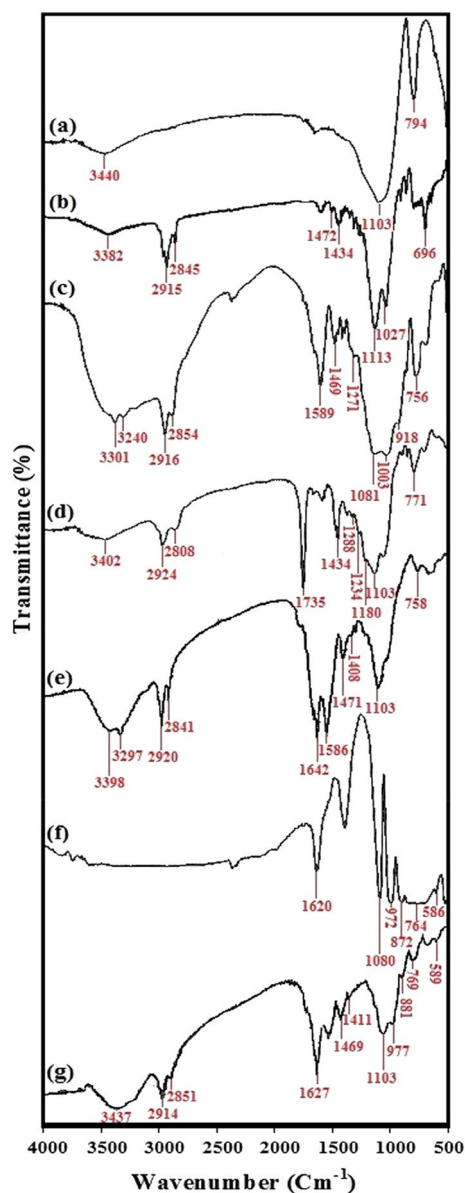
Fig. 1 FT-IR spectra *a* nSiO$_2$, *b* nSiO$_2$–Cl, *c* nSiO$_2$–NH$_2$, *d* P$_0$, *e* P$_{0.5}$, *f* PWA^n and *g* Dendrimer-PWA^n nanoparticles

Results and discussion

Catalyst characterization

FT-IR spectra of nSiO$_2$, nSiO$_2$–Cl, nSiO$_2$–NH$_2$, P$_0$, P$_{0.5}$, PWA^n and Dendrimer-PWA^n nanoparticles are shown in Fig. 1a–g. The bands centered around 3400 and 1620 cm^{-1} are, respectively, assigned to the O–H stretching and deforming vibrations of adsorbed water. The adsorption peaks at 1103 and 794 cm^{-1} corresponds to the antisymmetric and symmetric stretching vibration of Si–O–Si bond in oxygen-silica tetrahedron, respectively (Fig. 1a) [27].
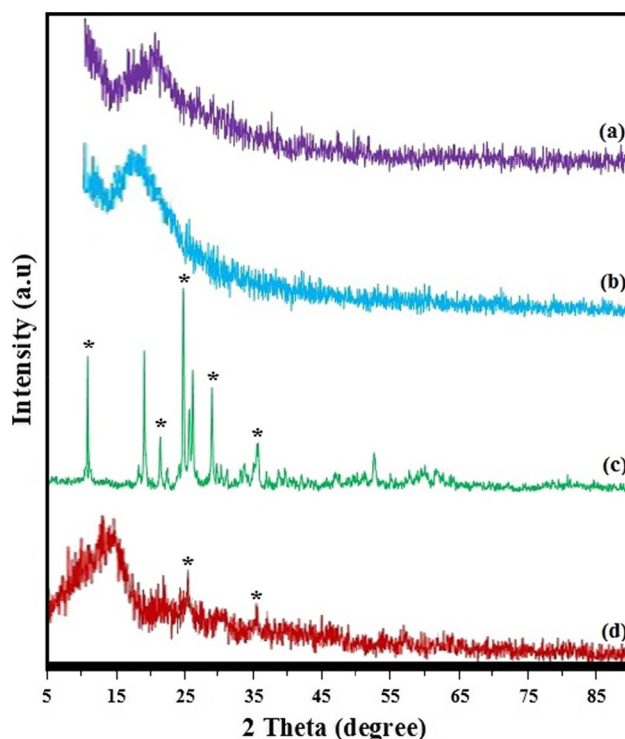
Fig. 2 XRD patterns of *a* nSiO$_2$, *b* P$_{1.5}$, *c* PWA^n and *d* Dendrimer-PWA^n nanoparticles

The presence of bands in the FT-IR spectra at 696 (C–Cl), 1000–1150 (Si–O–Si), 1472 (CH$_2$ bending) and 2845–2915 cm^{-1} (C–H$_{aliph}$) confirms the synthesis of nSiO$_2$–Cl (Fig. 1b) [31]. Figure 1c shows the FT-IR spectrum of n-SiO$_2$–NH$_2$ nanoparticles; the peaks at 1000–1150, 1271 and 1589 cm^{-1} are attributed to Si–O–Si (asymmetric stretching), C–N (stretching vibration) and N–H (bending), respectively [27]. Also, the absorption peaks in the regions 2854–2916 and 3100–3300 cm^{-1} are associated to C–H stretching of the methylene groups and N–H stretching (Fig. 1c). Complete conversion of amine (n–SiO$_2$–NH$_2$) to ester (P$_0$) and ester to amide (P$_{0.5}$) was proven by FT-IR spectra. Figure 1d shows the FT-IR spectrum of P$_0$ nanoparticles, the presence of absorbances at 2808–2924, 1735, 1288, 1234 and 1000–1150 are attributed to CH (stretching), C=O (ester stretching), C–O (stretching), C–N (stretching) and Si–O–Si, respectively [32]. From the IR spectra presented in Fig. 1e, the absorption peaks at 1642 cm^{-1} belonged to the stretching vibration mode of amide peaks in P$_{0.5}$ nanoparticles. Also, the presence of vibration bands in 3400 (O–H stretching), 3100–3300 (N–H stretching), 2841–2920 (C–H stretching), 1471 (CH$_2$ bending), 1241 (C–N) and 1000–1150 (Si–O–Si stretching) demonstrates the existence of P$_{0.5}$ nanoparticles in the spectrum (Fig. 1e) [32].

FT-IR spectroscopy, as a means of providing the structure of the HPAs, is convenient and widely is used for the characterization of heteropolyacids [18]. The FT-IR spectrum for PWA^n shows four bands in the range 500–1200 cm^{-1} that these bands are assigned at 764, 872, 972 and 1080 cm^{-1}, which are correspond to $\nu_{as}(W-O_e-W)$, $\nu_{as}(W-O_c-W)$, $\nu_{as}(W-O_t)$ and $\nu as(P-O^*)$, respectively [18]. It also shows a weak band in the region of 586 cm^{-1} that corresponds to the $\delta(P-O)$ vibration [18]. In the case of Dendrimer-PWA^n nanoparticles, the peak at 1080 cm^{-1} overlap with Si–O–Si stretching vibration, however, new peaks and non-overlapped bands at 977, 881 and 769 cm^{-1} are observed on FT-IR spectra of Dendrimer-PWA^n, indicating that PWA^n was anchored to $P_{1.5}$ successfully.

XRD analysis of the $nSiO_2$, $P_{1.5}$, PWA^n and Dendrimer-PWA^n nanoparticles is shown in Fig. 2. The diffraction peak which appeared at about $2\Theta = 10–20°$ in the structures is attributed to the amorphous silica gel (Fig. 2a, b, d) [33]. For $P_{1.5}$ and Dendrimer-PWA^n nanoparticles, the broad peak was transferred to lower angles due to the synergetic effect of amorphous silica and dendritic polymer (Fig. 2b, d). The strong characteristic peaks at $2\Theta = 10.55°$, $21.10°$, $25.95°$, $30.33°$ and $35.30°$ in Fig. 2c, are assigned to Keggin structure of PWA^n [JCPDS File 50-0657] [18]. Also, the XRD pattern of Dendrimer-PWA^n nanoparticles, showing the peaks of both amorphous silica and PWA^n and the diffraction peak at $25.95°$ and $35.30°$ indicates that PWA^n was anchored to $P_{1.5}$ successfully.

Morphology and structure of the synthesized materials were firstly investigated by TEM images. It is clear that the synthesized SiO_2 nanoparticles are well dispersed, but also in some areas bigger structures with non-spherical morphology are observed, more likely coming from aggregation of individual nanoparticles. The size distribution of these spheres is relatively uniform and their average diameter is 25 nm. Figure 3b displays the TEM image of PWA^n nanoparticles. The size of nanoparticles obtained from the TEM image, turned out to be approximately 30 nm for PWA^n, and their shape is nearly spherical. Figure 3c represented of TEM of Dendrimer-PWA^n nanoparticles. As illustrated, surface fictionalization of nanosilicate with dendritic polymer supported nano $H_3PW_{12}O_{40}$ caused nanoparticle aggregated and size of them arise to about 40 nm. In TEM image of these particles PWA^n nanoparticles clearly were seen (Fig. 3c). Also, to confirm if any aggregation of the PWA^n nanoparticles occurs, TEM analysis of the reused catalyst was performed (Fig. 3d). After six repeated reaction cycles, we did not observe significant change in the morphology of the catalyst, but some PWA^n particles might have aggregated onto the surfaces of the matrices. This may take place through the leaching/re-deposition processes during the catalytic reactions.

The hydrodynamic diameter of nanoparticles is determined by the DLS technique. This size distribution is centered at a value of 25, 30, 40 and 55 nm for $nSiO_2$, PWA^n, Dendrimer-PWA^n and Dendrimer-PWA^n after six cycles, respectively (Fig. 3e–h).

The presence of PWA^n species anchored on the support was also confirmed by UV–vis spectroscopy. Diffuse reflectance UV–visible spectra of $nSiO_2$, PWA^n and Dendrimer-PWA^n are shown in Fig. 4A. Nanosilica shows no absorption in the UV–vis region. PWA^n shows absorption band at 257 nm which is attributed to oxygen-tungsten charge transfer absorption bands for the Keggin anion [34]. On anchoring with $P_{1.5}$ nanoparticles, the 257 nm band is shifted to 263 nm reconforming the presence of PWA^n in $P_{1.5}$. According to the UV–vis analysis, PWA^n species indeed have been immobilized onto the support of $P_{1.5}$.

Figure 4B depicts the TGA results of nSiO2-Cl, nSiO2-NH2, P0, P0.5 and Dendrimer-PWAn.

TGA with heating from room temperature to 700 °C under a nitrogen atmosphere were conducted to determine the amount of organic composition in the modified silica nanoparticles. The TGA plots of samples depicted a two-step thermal decomposition.

According to Fig. 4B, the nanoparticles exhibit a weight loss in the range of 50–200 °C corresponding to the loss of physically adsorbed water and residual solvent from the surface of the silica nanoparticles, while weight loss between 200 and 430 °C was due to the removal of organic moieties on the surface [35].

The weight loss of Dendrimer-PWA^n NPs was 49.4 %, while only 5.7, 12.1, 21.4 and 31.6 % for $nSiO_2$-Cl, $nSiO_2$-NH_2, P_0 and $P_{0.5}$ NPs over the whole temperature range (Fig. 4B a–e).

The textural properties of n-SiO_2 and Dendrimer-PWA^n were evaluated from the nitrogen adsorption–desorption isotherms (Fig. 4C) and the respective specific surface area (BET method), pore volume (BJH method) and average pore radius were calculated.

It can be clearly seen that N_2 adsorption–desorption isotherms of n-SiO_2 and Dendrimer-PWA^n all show representative type-IV curves with type H1 hysteresis loops, indicating the presence of textual mesopores. The average pore radius of n-SiO_2 is 10.2 nm, and its BET surface area and pore volume are calculated to be 531 and 1.3 cm^3 g^{-1}, respectively. After dendrimer encapsulated PWA^n functionalization, the average pore radius, BET surface area, and pore volume of Dendrimer-PWA^n decrease to 6.1 nm, 479 m^2 g^{-1}, and 0.6 cm^3 g^{-1}, respectively. This indicates that pore volume decreases upon grafting of dendritic polymer molecules within the pore structure or in other words thickness of pore wall increases.

Fig. 3 TEM images of: **a** nSiO$_2$, **b** PWA^n, **c** Dendrimer-PWA^n and **d** Dendrimer-PWA^n after six cycles; particle size distribution results for **e** nSiO$_2$, **f** PWA^n, **g** Dendrimer-PWA^n and **h** Dendrimer-PWA^n after six cycles
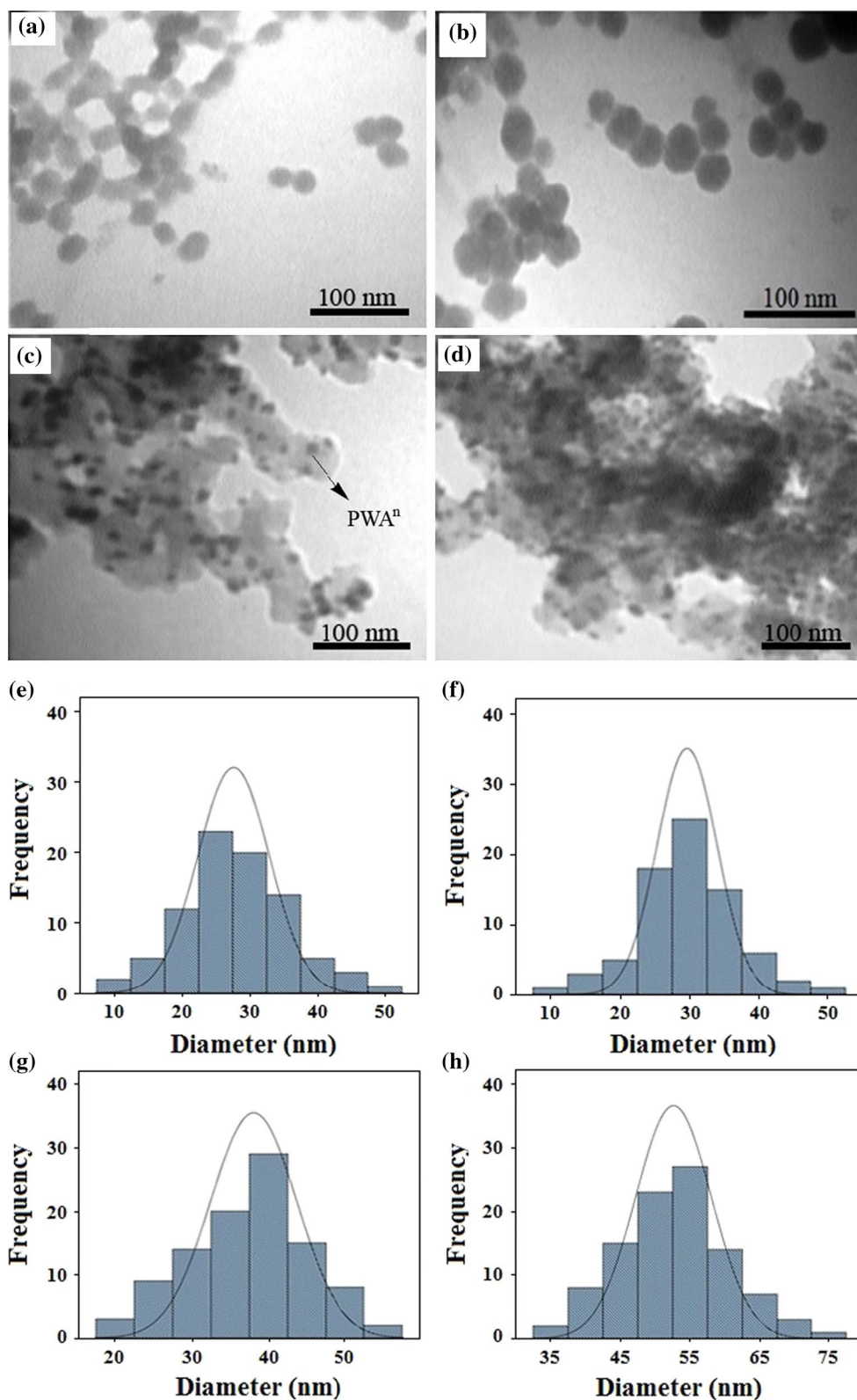
Brönsted or Lewis acidity of the Dendrimer-PWA^n catalyst was distinguished by studying the FTIR spectrum of the catalyst after reaction with pyridine (Fig. 4D).

Pyridine molecules were adsorbed on Lewis acid sites (1610 and 1450 cm^{-1}) and formed the pyridinium ion by interaction with Brönsted acid sites (1640 and 1540 cm^{-1})
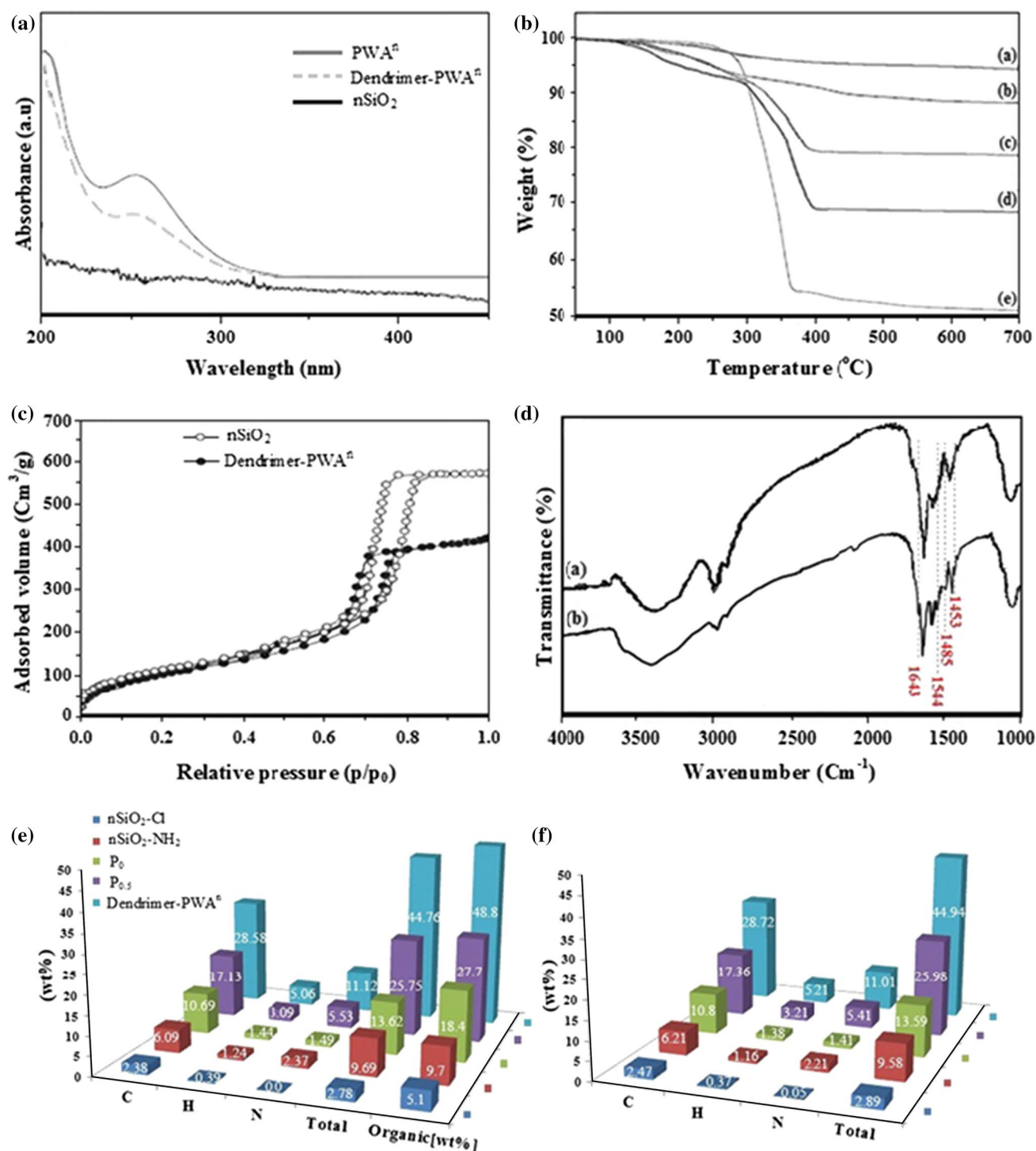
Fig. 4 **A** UV–Vis spectra of nSiO$_2$, PWA^n and Dendrimer-PWA^n; **B** Thermogravimetric analysis of *a* n-SiO$_2$–Cl, *b* n-SiO$_2$–NH$_2$, *c* P$_0$, P$_{0.5}$ and Dendrimer-PWA^n nanoparticles; **C** Nitrogen adsorption–desorption isotherms of *n*SiO$_2$, and Dendrimer-PWA^n; **D** FT-IR spectra *a* Dendrimer-PWA^n, and pyridine adsorption of *b* Dendrimer-PWA^n, **E** TGA and **F** elemental analysis (EA) results for the synthesis of Dendrimer-PWA^n nanoparticles

[18]. Both types of adsorbed species contribute to the band at 1490 cm^{-1}. The formation of pyridinium ion was observed by absorptions at 1485, 1544 and 1643 cm^{-1} (Fig. 4D b). It should be mentioned that absorption band at 1643 cm^{-1} is not totally conclusive although considered as pyridinium ion because of contributions of pyridinium

ion and moisture, since the spectrum was taken at ambient conditions.

A summary of the TGA and elemental analysis data is included in Fig. 4. A good agreement was observed between elemental analysis and TGA data for these conversions.

Also, in this article, determination of PWA^n content was performed by inductively coupled plasma-atomic emission spectroscopy (ICP-AES). According to the ICP-AES analysis, the amounts of PWA^n immobilized on nanosilica supported dendritic polymer was found to be 39.7 wt % (0.14 mmol/g).

Synthesis of 2*H*-indazolo[2,1-*b*]phthalazine-triones in the presence of Dendrimer-PWA^n catalyst

Due to ability of Dendrimer-PWA^n as a mild and efficient acid catalyst, we decided to apply this catalyst for synthesis of 2*H*-indazolo[1,2-*b*] phthalazine-triones.

Initially to obtain the best reaction conditions, the reaction of benzaldehyde (1 mmol), dimedone (1 mmol), hydrazinium hydroxide (1.2 mmol) and phthalic anhydride (1 mmol) was chosen as a model reaction. The model reaction was refluxed in the presence of 0.14 mol % of Dendrimer-PWA^n and a variety of solvents such as H_2O, EtOH, EtOH:H_2O [1/1(v/v)], DMF, CH_2Cl_2 and CH_3CN. The represented data in Table 1 showed the corresponding products were obtained in 66, 68, 51, 62, 33, and 56 % yield, respectively, after 1 h (Table 1, entries 1–5 and 7). We also checked the model reaction in refluxing toluene as a solvent in the presence of 0.14 mol % of Dendrimer-PWA^n and the corresponding products were obtained in 44 % yield (Table 1, entry 6). As it was shown in Table 1 the best result was obtained when the model reaction was carried out under solvent-free condition in the presence of 0.14 mol % of Dendrimer-PWA^n at 80 °C and the desired product was obtained in high yields after 10 min (Table 1, entry 8). The model reaction was also examined in absent of catalyst under solvent-free conditions at 100 °C and the reaction did not proceed even after 3 h (Table 1, entry 9).

Then we decided to check the model reaction under solvent-free condition at 80 °C and various amount of catalyst. As it was shown in Table 1 the best result was obtained when we carried out the model reaction in the presence of 0.14 mol % of catalyst. This condensation was carried out with low amounts of Dendrimer-PWA^n of 0.07 and

Table 1 Optimization of the amount of catalyst, solvent and temperature in a one-pot four-component synthesis of the model reaction

Entry	Catalyst amount (mol %)	Solvent	Condition	Time (min)	Yield (%)[a]
1	0.14	EtOH	Reflux	60	68
2	0.14	EtOH-H_2O [50/50(v/v)]	Reflux	60	51
3	0.14	DMF	120 °C	60	62
4	0.14	CH_3CN	Reflux	60	56
5	0.14	CH_2Cl_2	Reflux	60	33
6	0.14	Toluene	Reflux	120	44
7	0.14	H_2O	Reflux	60	66
8	0.14	Solvent-free	80 °C	10	93
9	None	Solvent-free	100 °C	180	–
10	0.07	Solvent-free	80 °C	30	77
11	0.11	Solvent-free	80 °C	15	88
12	0.17	Solvent-free	80 °C	10	92
13	0.20	Solvent-free	80 °C	10	90
14	0.14	Solvent-free	rt	60	34
15	0.14	Solvent-free	50 °C	30	83
16	0.14	Solvent-free	70 °C	20	90
17	0.14	Solvent-free	90 °C	10	92
18	None	Solvent-free	)))), rt	60	–
19	0.07	Solvent-free	)))), rt	60	56
20	0.14	Solvent-free	)))), rt	20	74
21	0.18	Solvent-free	)))), rt	10	87
22	0.21	Solvent-free	)))), rt	10	94
23	0.25	Solvent-free	)))), rt	15	94

Reaction conditions benzaldehyde (1 mmol), dimedone (1 mmol), hydrazinium hydroxide (1.2 mmol), phthalic anhydride (1 mmol), Dendrimer-PWA^n catalyst and solvent (3 mL)

[a] Isolated yield

0.11 mol % and the corresponding products were obtained in longer reaction times and lower yields (Table 1, entries 10 and 11). On the other hand, higher amounts of catalyst did not improve the yield or reaction time (Table 1, entries 12, 13). The effect of temperature was also studied by carrying out the model reaction in the presence of 0.14 mol % of catalyst at RT, 50, 70 and 90 °C under solvent-free condition. It was observed that the corresponding products were obtained in 34, 83, 90 and 92 % yield, respectively (Table 1, entries 14–17).

Considering the ability of ultrasonic irradiation for the acceleration of organic reactions, we examined the model reaction under ultrasonic irradiation and solvent-free condition at room temperature in presence of various amount of catalyst. As it is clear from Table 1, the best results were obtained in the presence of 0.21 mol % of catalyst (Table 1, entry 22).

However, synthesis of organic compounds under ultrasound irradiation has been limited by the need for a specialized apparatus that may not be available in many laboratories. Because of this limitation, herein we report both ultrasonic irradiation in presence of 0.21 mol % of catalyst at room temperature and solvent-free condition in the presence of 0.14 mol % of catalyst at 80 °C (Table 1, entries 22 and 8) for the synthesis of 2H-indazolo[1,2-b] phthalazine-triones.

After optimizing the reaction conditions, the generality of this catalytic system was confirmed by the employment of a series of aldehydes, dimedone, hydrazinium hydroxide and phthalic anhydride to obtain desired products under the optimized conditions. The results are summarized in Table 2.

As it is shown in Table 2, based on the optimized reaction conditions, we studied the reaction with a wide range of aromatic aldehydes with electron donating and electron withdrawing groups. Both electron-rich and electron-deficient aldehydes worked well and give high yields of products under both solvent-free and ultrasonic irradiation in short reaction times. Thus, the nature and position of substitution in the aromatic ring did not affect the reactions much (Table 2, entries 2–19).

Also both of our methodologies have been successfully used for heteroaromatic aldehydes that are acid sensitive species such as thiophene-2-carbaldehyde, 5-bromothiophene-2-carbaldehyde, indole-3-carbaldehyde and pyridyne-2-carbaldehyde and the corresponding products were obtained in excellent yields without the formation of any byproduct (Table 2, entries 21–24). We also checked aliphatic aldehydes (Table 2, entries 25–27), the yields were quite reasonable. Aliphatic aldehydes gave the corresponding product in moderate yield and required more reaction time, probably due to the low reactivity of aliphatic aldehydes in compare with aromatics.

A proposed mechanism for the synthesis of 2H-indazolo [2,1-b] phthalazine-triones outlined in Scheme 2. Based on this mechanism, as shown in Scheme 2, the reaction occurs in step 1 via initial formation of the phthalhydrazide by nucleophilic addition of hydrazinium hydroxide to phthalic anhydride followed by dehydration. The second step involves initial formation of heterodyne by standard Knoevenagel condensation of dimedone and aldehyde. Subsequent Michael-type addition of the phthalhydrazide followed by cyclization affords the corresponding product [41] (Scheme 2).

To compare the reactivity of the Dendrimer-PWA^n with previously reported catalysts, a comparative chart is presented in Table 3. Although, all the catalysts listed in Table 3 were able to produce good yields of corresponding products, however some of these reactions were carried out under harsh reaction conditions such as toxic solvents and high temperature (Table 3, entries 5 and 9). Some of these need very long reaction time (Table 3, entry 12). Moreover, some of the catalysts listed in Table 3 are not reusable. Thus, our reusable catalyst and green methodologies have been established as a better alternative compared to the reported methods for the fabrication of corresponding products.

The reusability and recovery of the catalyst are important issues, especially when the reactions use solid catalysts. Thus, the recovery and reusability of catalyst were investigated for the preparation of 3,4-dihydro-3,3-dimethyl-13-phenyl-2H-indazolo[2,1-b]phthalazine-1,6,11(13H)-trione (5a) under ultrasound irradiation at room temperature and solvent-free conditions at 80 °C (Fig. 5). The catalyst was recovered after each run, washed with hot ethanol (2 × 10 mL), dried in an oven at 60 °C for 180 min prior to use and tested for its activity in the subsequent run. The performance of the recycled catalyst in reaction up to six successive runs was shown in Fig. 5. These bar diagrams clearly suggest that the desired products were obtained in high yields without distinct deterioration in catalytic activity.

To determine the degree of leaching of the metal from the heterogeneous catalyst, the catalyst was removed by using a magnetic field and the Tungsten (W) amount in reaction medium after each reaction cycle was measured through Inductively Coupled Plasma (ICP) analyzer. The amount of W leaching after the first run was determined by ICP analysis to be only 0.28 %, and after six repeated recycling was 4.34 %. Therefore, the analysis of the reaction mixture by the ICP technique showed that the leaching of $H_3PW_{12}O_{40}$ was negligible.

Table 2 One-pot four-component synthesis of 2*H*-indazolo[2,1-*b*]phthalazine-1,6,11(13H)-trione derivatives catalyzed by Dendrimer-PWA[n]
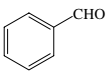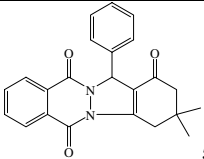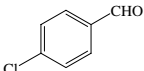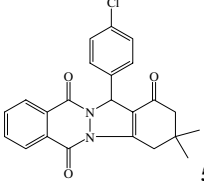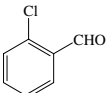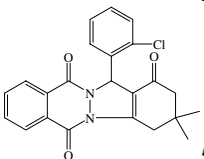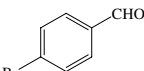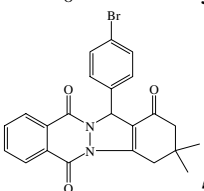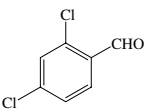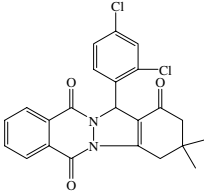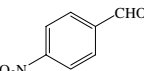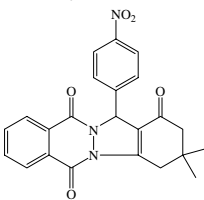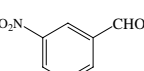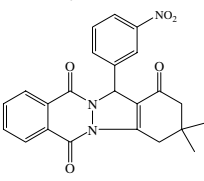
Entry	Aldehyde	Product	Solvent-free/80°C		Ultrasonic/r.t		M.p. °C (Lit.)
			Time (min)	Yield (%)[b]	Time (min)	Yield (%)[b]	
1	CHO (benzaldehyde)	**5a**	10	93	10	94	204-205 (206-208)[36]
2	CHO (4-Cl)	**5b**	10	92	10	91	260-261 (260-262)[37]
3	CHO (2-Cl)	**5c**	15	89	15	90	267-268 (266-267)[36]
4	CHO (4-Br)	**5d**	18	91	10	88	264-265 (265-267)[10]
5	CHO (2,4-diCl)	**5e**	15	94	8	95	218-220 (219-221)[9]
6	CHO (4-NO₂)	**5f**	10	95	10	94	217-218 (215-217)[36]
7	CHO (3-NO₂)	**5g**	10	90	15	87	268-270 (269-272)[38]

Table 2 continued
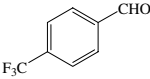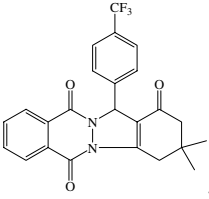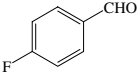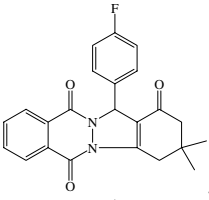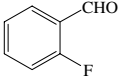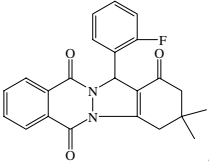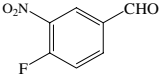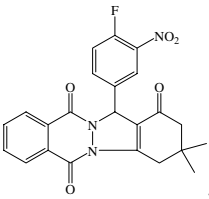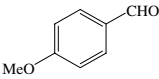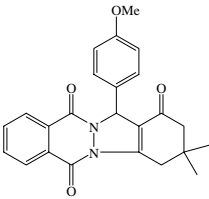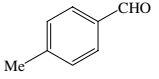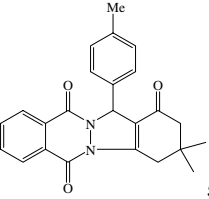
Entry	Aldehyde	Product	Solvent-free/80°C		Ultrasonic/r.t		M.p. °C (Lit.)
			Time (min)	Yield (%)[b]	Time (min)	Yield (%)[b]	
8		5h	12	88	10	90	216 (214-216)[36]
9		5i	15	92	12	89	219-221 (221-222)[37]
10		5j	15	86	10	88	268-269 (270-272)[39]
11		5k	10	93	10	94	226-228 (225-227)[11]
12		5l	15	90	12	87	220-222 (218-220)[36]
13		5m	20	91	20	89	229-230 (227-229)[36]

Table 2 continued
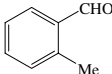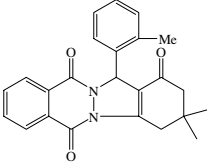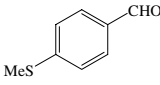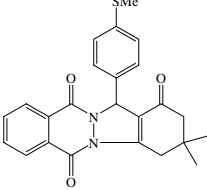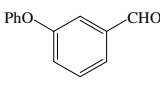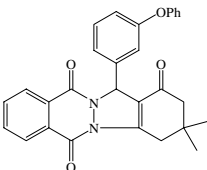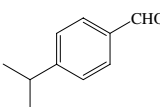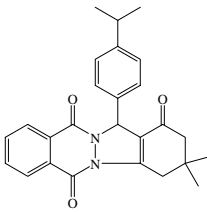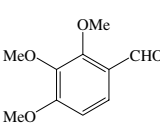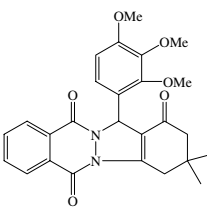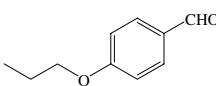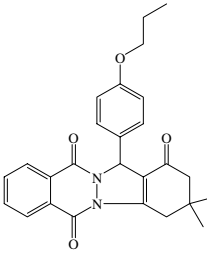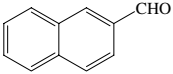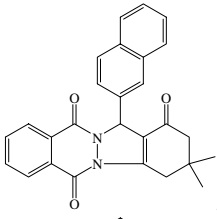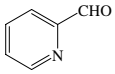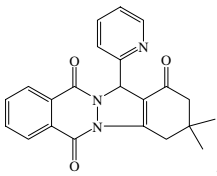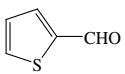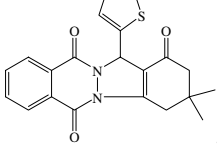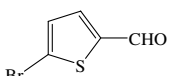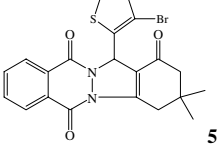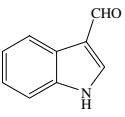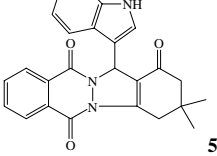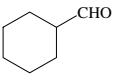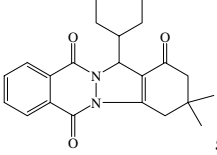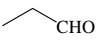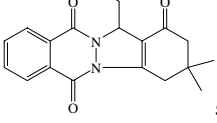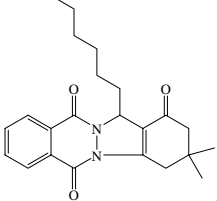
Entry	Aldehyde	Product	Solvent-free/80°C		Ultrasonic/r.t		M.p. °C (Lit.)
			Time (min)	Yield (%)[b]	Time (min)	Yield (%)[b]	
14		**5n**	25	88	20	91	238-240 (239-241)[36]
15		**5o**	10	91	12	93	230-232 (230-231)[37]
16		**5p**	15	93	10	91	185-186 (183-185)[36]
17		**5q**	12	87	15	85	229-230 (230-232)[36]
18		**5r**	20	86	15	89	185-187
19		**5s**	15	92	10	90	160-162

Table 2 continued

Entry	Aldehyde	Product	Solvent-free/80°C		Ultrasonic/r.t		M.p. °C (Lit.)
			Time (min)	Yield (%)[b]	Time (min)	Yield (%)[b]	
20	CHO (naphthalene)	5t	10	92	12	91	249-251 (250-252)[40]
21	CHO (pyridine)	5u	10	89	8	92	231-232 (230-232)[37]
22	CHO (thiophene)	5v	15	93	10	90	219-220
23	Br-thiophene-CHO	5w	10	88	12	91	205-207
24	CHO (indole)	5x	18	91	20	93	250-251 (248-250)[36]
25	CHO (cyclohexane)	5y	25	86	20	87	219-221 (220-222)[37]
26	CHO (propanal)	5z	30	74	20	78	145-147 (146-148)[40]
27	$CH_3(CH_2)_5CHO$	5aa	30	77	25	73	84-86 (82-85)[9]

Reaction conditions aldehyde (1 mmol), dimedone (1 mmol), hydrazinium hydroxide (1.2 mmol), phthalic anhydride (1 mmol), Dendrimer-PWA[n] catalyst (0.14 mol %/solvent-free/80 °C, 0.21 mol %/ultrasonic/r.t)

[a] Isolated yield
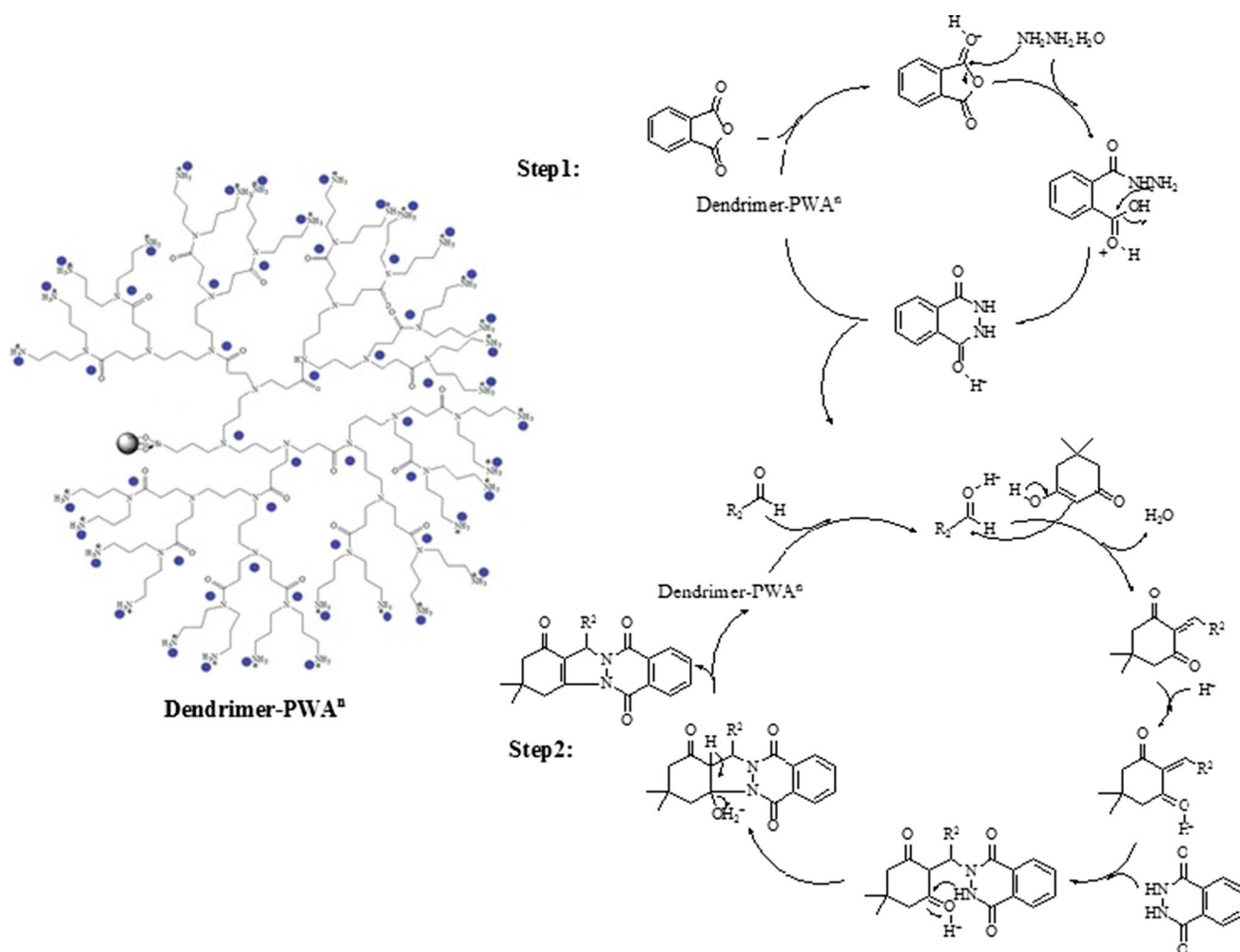
Scheme 2 Suggested mechanism for the synthesis of 2*H*-indazolo[2,1-*b*]phthalazine-triones in the presence of Dendrimer-PWA[n] catalyst

Conclusion

In summary, we report for the first time a novel kind of dendrimer-encapsulated phosphotungstic acid nanoparticles immobilized on nanosilica with surface amino groups. The catalyst was successfully synthesized and structural, surface and morphological of these nanoparticles were evaluated. TEM indicate that the silica nanoparticles have been well-coated with dendrimer-encapsulated phosphotungstic acid nanoparticles. The crystallite size obtained from X-ray line profile fitting is comparable with the particle size obtained from TEM. The FT-IR and TGA results demonstrated the formation of Dendritic Polymer in the presence of the SiO_2 NPs. Therefore, the Dendrimer-PWA[n] is synthesized and can efficiently catalyze the green synthesis of 2*H*-indazolo[1,2-*b*] phthalazine-triones via a one-pot, four-component condensation reaction of aldehydes, phthalic anhydride, hydrazinium hydroxide, and dimedone under solvent-free ultrasound irradiation at room temperature as well as solvent-free conditions at 80 °C. The attractive features of this protocol are high catalytic activity, thermal stability, heterogeneous nature of the catalyst, operational simplicity, cleaner reactions, reduced reaction times, eco-friendly promising strategy, satisfactory yields of products, lower loading of catalyst compared with the other methods, and avoidance of using hazardous organic solvents that makes this method an instrumental alternative to the previous methodologies for the scale up of these one-pot four-component reactions. In addition, the catalyst could be successfully recycled and reused at least for six runs without significant loss in activity.

Table 3 Comparison of our results with previously reported methods

Entry	Catalyst	Conditions	Time (min)	Yield (%)[a]	Ref.
1	Mg(HSO$_4$)$_2$[b]	Solvent-free/100 °C	10	85	[42]
2	PMA–SiO$_2$[b]	Solvent-free/80 °C	30	85	[39]
3	Nano-alumina sulfuric acid[b]	Solvent-free/110 °C	14	85	[43]
4	Ce(SO$_4$)$_2$.4H$_2$O[c]	Solvent-free/125 °C	6	78	[41]
5	PBBS[b]	Solvent-free/100 °C	25	65	[9]
6	[TMG][Ac][c]	Solvent-free/80 °C	15	92	[40]
7	TMSCl[b]	Reflux/CH$_3$CN/DMF	30	86	[38]
8	PEG-OSO$_3$H[c]	Solvent-free/80 °C	13	87	[44]
9	hexafluoro-2-propanol[b]	Solvent-free/55 °C	480	92	[45]
10	H$_2$SO$_4$[b]	[bmim]BF$_4$/80 °C	35	91	[46]
		H$_2$O-EtOH/Reflux	30	88	[46]
11	(S)-camphorsulfonic acid[b]	Solvent-free/80 °C	15	90	[10]
		Ultrasonic/r.t	20	87	[10]
12	[Bmim]Br[c]	Ultrasonic/r.t	10	93	[47]
13	Dendrimer-PWA[n]	Solvent-free/80 °C	10	93	This work
		Ultrasonic/r.t	10	94	This work

[a] Yields refer to the isolated pure products

[b] Based on the reaction of benzaldehyde, dimedone and phthalhydrazide

[c] Based on the reaction of benzaldehyde, dimedone, phthalic anhydride and hydrazinium hydroxide
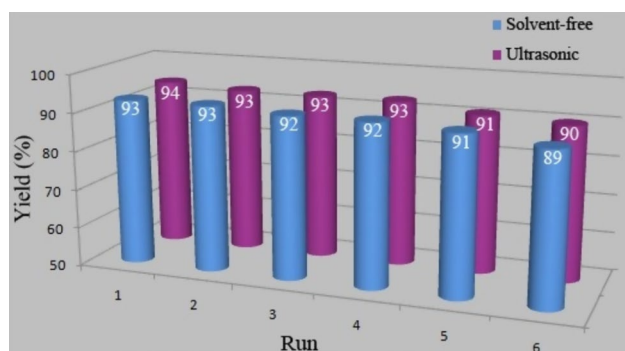
Fig. 5 Recyclability of Dendrimer-PWA[n] in the synthesis of **5a** under the optimized conditions

Selected spectral data

3,4-Dihydro-3,3-dimethyl-13-phenyl-2H-indazolo[2,1-b] phthalazine-1,6,11(13H)-trione (5a)

Yellow Powder, M.P. = 204–205 °C, ^{1}H NMR (500 MHz, CDCl$_3$) δ: 1.23 (s, 6H), 2.36 (s, 2H), 3.27 (dd,1H, J = 19.01 Hz and 2.07 Hz), 3.44 (d, 1H, J = 19.01 Hz), 6.4 (s, 1H), 7.29–7.37 (m, 5H), 7.44 (d, 2H, J = 7.2 Hz), 7.86–7.87 (m, 2H), 8.28–8.36 (m, 2H); ^{13}C NMR (125 MHz, CDCl$_3$) δ: 28.9, 29.1, 35.0, 38.4, 51.3, 95.4, 119.0, 127.5, 128.2, 128.4, 129.1, 129.4, 129.5, 133.9, 134.9, 136.8, 151.2, 154.7, 156.4, 192.5; IR (KBr, cm^{-1}): 2952, 1667, 1578, 1356, 1304, 1271; Anal. Calcd for C$_{23}$H$_{20}$N$_2$O$_3$: C, 74.18; H, 5.41; N, 7.52 %, Found: C, 74.11; H, 5.47; N, 7.57 %.

3,4-Dihydro-3,3-dimethyl-13-(4-chlorophenyl)-2H-indazolo[2,1-b]phthalazine-1,6,11(13H)-trione (5b)

White powder, M.P. = 260–261 °C, ^{1}H NMR (500 MHz, CDCl$_3$) δ: 1.23 (s, 6H), 2.36 (s, 2H), 3.26 (d, 1H, AB system, J = 18.90 Hz), 3.43 (d, 1H, AB system, J = 18.84 Hz), 6.44 (s, 1H), 7.29-7.37 (m, 4H), 7.88–7.90 (m, 2H), 8.30–8.38 (m, 2H). ^{13}C NMR (125 MHz, CDCl$_3$) δ: 28.5, 28.7, 34.7, 38.0, 50.9, 64.3, 118.1, 127.7, 128.1, 128.5, 128.8, 128.9, 129.0, 133.7, 134.5, 134.6, 134.9, 151.1, 154.3, 156.0, 192.2; IR (KBr, cm^{-1}): 2960, 1665, 1628, 1361, 1313, 1264, 786; Anal. Calcd for C$_{23}$H$_{19}$ClN$_2$O$_3$: C, 67.90; H, 4.71; N, 6.89 %, Found: C, 67.94; H, 4.65; N, 6.81 %.

3,4-Dihydro-3,3-dimethyl-13-(2-chlorophenyl)-2H-indazolo[2,1-b]phthalazine-1,6,11(13H)-trione (5c)

Yellow powder, M.P. = 267–268 °C, ^{1}H NMR (500 MHz, CDCl$_3$) δ: 1.23 (s, 6H), 2.34 (s, 2H), 3.26 (d, 1H, AB system, J = 18.98 Hz), 3.42 (d, 1H, AB system, J = 19.00 Hz), 6.7 (s, 1H), 7.24-7.50 (m, 4H), 7.87-8.39 (m, 4H); ^{13}C NMR (125 MHz, CDCl$_3$) δ: 28.8, 29.2, 35.0, 38.4, 51.3, 64.4, 116.7, 127.6, 128.1, 128.4, 129.1, 129.4, 130.2, 130.9, 132.0, 133.0, 133.9, 134.9, 152.2, 154.6, 156.6, 192.4; IR (KBr, cm^{-1}): 2957, 1661, 1622, 1467, 1472, 1359, 1311, 1267, 791; Anal. Calcd for C$_{23}$H$_{19}$ClN$_2$O$_3$: C, 67.90; H, 4.71; N, 6.89 %, Found: C, 67.83; H, 4.66; N, 6.94 %.

3,4-Dihydro-3,3-dimethyl-13-(4-bromophenyl)-2H-indazolo[2,1-b]phthalazine-1,6,11(13H)-trione (5d)

White powder, M.P. = 264-265 ∘C, ^{1}H NMR (500 MHz, CDCl$_3$) δ: 1.23 (s, 6H), 2.36 (s, 2H), 3.26 (d, 1H, AB system, J = 19.02 Hz), 3.42 (d, 1H, AB system, J = 19.00 Hz), 6.42 (s, 1H), 7.29–7.4 (m, 4H), 7.8–8.3 (m, 4H). ^{13}C NMR (125 MHz, CDCl$_3$) δ: 28.5, 28.7, 34.7, 38.0, 50.9, 64.4, 118.0, 122.8, 127.8, 128.1, 128.8, 128.9, 129.0, 131.9, 133.7, 134.7, 135.5, 151.1, 154.4, 156.0, 192.1; IR (KBr, cm^{-1}): 2957, 1656, 1623, 1573, 1471, 1308, 1267; Anal. Calcd for C$_{23}$H$_{19}$BrN$_2$O$_3$: C, 61.21; H, 4.24; N, 6.21 %, Found: C, 61.13; H, 4.29; N, 6.27 %.

4.2.5. 3,4-Dihydro-3,3-dimethyl-13-(2,4-dichlorophenyl)-2H-indazolo[2,1-b]phthalazine-1,6,11(13H)-trione (5e):

Yellow powder, M.P. = 218–220 °C, ^{1}H NMR (500 MHz, CDCl$_3$) δ: 1.21 (s, 3H), 1.23 (s, 3H), 2.33 (s, 2H), 3.20–3.44 (2H, AB system, J = 19.2 Hz), 6.64 (s, 1H), 7.26–8.42 (m, 7H); ^{13}C NMR (125 MHz, CDCl$_3$) δ: 28.4, 28.7, 34.6, 38.0, 50.8, 63.5, 118.1, 127.6, 127.7 (2C), 128.1, 128.6, 129.0, 131.1, 131.7, 133.2, 133.7, 134.6, 135.1, 152.0, 154.3, 156.1, 192.1; IR (KBr, cm^{-1}): 2967, 1664, 1627; 1473, 1369, 1253, 772; Anal. Calcd for C$_{23}$H$_{18}$Cl$_2$N$_2$O$_3$: C, 62.60; H, 4.10; N, 6.35 %, Found: C, 62.71; H, 4.16; N, 6.31 %.

3,4-Dihydro-3,3-dimethyl-13-(4-nitrophenyl)-2H-indazolo[2,1-b]phthalazine-1,6,11(13H)-trione (5f)

Yellow powder, M.P. = 217–218 °C, ^{1}H NMR (500 MHz, CDCl$_3$) δ: 1.21 (s, 3H), 1.24 (s, 3H), 2.1 (s, 2H), 3.2 (dd, 1H, AB system, J = 19.10 Hz, J = 2.23 Hz), 3.43 (d, 1H, AB system, J = 19.21 Hz), 6.53 (s, 1H), 7.61–7.64 (m, 2H), 7.90–7.91 (m, 2H), 8.20–8.41 (m, 4H); ^{13}C NMR (125 MHz, CDCl$_3$) ı: 28.8, 29.1, 31.3, 35.1, 38.4, 51.2, 64.5, 117.7, 128.2, 128.4, 128.6, 129.1, 129.3, 134.3, 135.2, 143.8, 148.3, 152.1, 154.9, 156.3, 192.4. %. IR (KBr, cm^{-1}): 2973, 1697, 1617, 1660, 1525, 1368, 1148, 1102, 858, 701; Anal. Calcd for C$_{23}$H$_{19}$N$_3$O$_5$: C, 66.18; H, 4.59; N, 10.07 %, Found: C, 66.23; H, 4.55; N, 10.03 %.

3,4-Dihydro-3,3-dimethyl-13-(3-nitrophenyl)-2H-indazolo[2,1-b]phthalazine-1,6,11(13H)-trione (5 g)

Yellow powder, M.P. = 268–270 °C, ^{1}H NMR (500 MHz, CDCl$_3$) δ: 1.2 (s, 6H), 2.38 (s, 2H), 3.30 (dd, 1H, AB system, J = 19.15 Hz, J = 2.12 Hz), 3.46 (d, 1H, AB system, J = 19.20 Hz), 6.5 (s, 1H), 7.59 (t, 1H, J = 7.84 Hz), 7.89–7.93 (m, 3H), 8.19 (d, 2H, J = 8.75 Hz), 8.26–8.42 (m, 2H); ^{13}C NMR (125 MHz, CDCl$_3$) δ: 28.8, 29.1, 35.1, 38.4, 51.2, 64.6, 117.6, 121.9, 124.1, 128.1, 128.7, 129.1, 129.4, 130.1, 134.3, 134.6, 135.2, 139.05, 152.2, 192.5. (KBr, cm^{-1}): 2926, 1660, 1625, 1516, 1374, 1147, 1107,

867, 697; Anal. Calcd for C$_{23}$H$_{19}$N$_3$O$_5$: C, 66.18; H, 4.59; N, 10.07 %, Found: C, 66.23; H, 4.66; N, 10.04 %.

3,4-Dihydro-3,3-dimethyl-13-(4-fluorophenyl)-2H-indazolo[2,1-b]phthalazine-1,6,11(13H)-trione (5i)

Yellow powder, M.P. = 219–221 °C, ^{1}H NMR (500 MHz, CDCl$_3$) δ: 1.24 (s, 6H), 2.36 (s, 2H), 3.26 (dd, 1H, AB system, J = 19.06 Hz, J = 2.21 Hz), 3.43 (dd, 1H, AB system, J = 19.34 Hz, J = 1.20 Hz), 6.46 (s, 1H), 7.02–7.06 (m, 2H), 7.40–7.44 (m, 2H), 7.86-7.89 (m, 2H), 8.27–8.39 (m, 2H); ^{13}C NMR (125 MHz, CDCl$_3$) δ: 28.8, 29.1, 35.1, 38.4, 51.3, 64.7, 116.0, 116.2 (d, J_{C-F} = 276 Hz), 118.6, 128.1, 128.4, 129.3, 129.4, 132.6, 134.0, 135.0, 151.4, 154.8, 156.4, 162.1, 164.1, 192.5; IR (KBr, cm^{-1}): 2958, 2867, 1664, 1655, 1626; 1473, 1309; Anal. Calcd for C$_{23}$H$_{19}$FN$_2$O$_3$: C, 70.76; H, 4.91; N, 7.18 %, Found: C, 70.69; H, 4.85; N, 7.09 %.

3,4-Dihydro-3,3-dimethyl-13-(2-fluorophenyl)-2H-indazolo[2,1-b]phthalazine-1,6,11(13H)-trione (5j)

Yellow powder, M.P. = 268–269 °C, ^{1}H NMR (500 MHz, CDCl$_3$) δ: 1.18 (s, 3H), 1.22 (s, 3H), 2.31 (s, 2H), 3.41, 3.22 (2H, AB System, J = 19.06 Hz,), 6.54 (s, 1H), 7.01 (t, 1H, J = 10.36 Hz), 7.14 (t, 1H, J = 7.63 Hz), 7.26–7.31 (q, 1H), 7.44 (t, 1H, J = 7.31 Hz), 7.87–7.89 (m, 2H), 8.19–8.21 (m, 1H), 8.33–8.35 (m, 1H); ^{13}C NMR (125 MHz, CDCl$_3$) δ: 27.2, 28.0, 33.8, 37.1, 50.0, 59.7, 114.9, 115.9, 123.5, 126.5, 127.2, 127.9, 128.2, 129.4, 129.5, 132.8, 133.7, 150.8, 153.3, 155.0, 159.2, 191.1; IR (KBr, cm^{-1}): 2951, 2868, 1665, 1621, 1354, 1311.

3,4-Dihydro-3,3-dimethyl-13-(4-fluoro-3-nitrophenyl)-2H-indazolo[2,1-b]phthalazine-1,6,11(13H)-trione (5k)

Yellow powder, M.P. = 226–228 ∘C, ^{1}H NMR (500 MHz, CDCl$_3$) δ: 1.22 (s, 6H), 2.35 (s, 2H), 3.42, 3.26 (2H, AB system, J = 19.25 Hz,), 6.46 (s, 1H), 7.30 (d, 1H, J = 8.50 Hz), 7.87–7.90 (m, 3H), 8.02 (dd, 1H, J = 9.25, 2.02 Hz,), 8.23–8.26 (m, 1H), 8.36–8.38 (m, 1H); ^{13}C NMR (125 MHz, CDCl$_3$) δ: 28.4, 28.7, 34.7, 37.9, 50.7, 63.5, 116.7, 118.6, 118.8, 124.3, 127.6, 128.5, 128.9, 133.6, 133.9, 134.8, 135.2, 151.9, 154.7, 155.9, 192.1; IR (KBr, cm^{-1}): 2956, 2873, 1654, 1321, 1273.

3,4-Dihydro-3,3-dimethyl-13-(4-methoxyphenyl)-2H-indazolo[2,1-b]phthalazine-1,6,11(13H)-trione (5l)

Yellow powder, M.P. = 220–222 °C, ^{1}H NMR (500 MHz, CDCl$_3$) δ: 1.23 (s, 3 H), 1.24 (s, 3 H), 2.30 (s, 2 H), 3.21, 3.42 (2 H, AB system, J = 18.95), 3.75 (s, 3 H), 6.38 (s, 1 H), 6.35–8.80 (m, 8H); ^{13}C NMR (125 MHz, CDCl$_3$) δ:

28.4, 28.7, 34.6, 38.1, 50.9, 55.1, 64.5, 114.1, 118.5, 127.6, 127.9, 128.3, 128.5, 128.9, 129.1, 133.4, 134.9, 1507, 154.2, 156.0, 159.6, 192.2; IR (KBr, cm^{-1}): 2957, 1665, 1627, 1602, 1511, 1467, 1427, 1360, 1314, 1266, 1243, 1170, 1101, 1029, 842, 799, 701.

3,4-Dihydro-3,3-dimethyl-13-(4-methylphenyl)-2H-indazolo[2,1-b]phthalazine-1,6,11(13H)-trione (5m)

Yellow powder, M.P. = 229–230 ∘C, ^{1}H NMR (500 MHz, CDCl$_3$) δ: 1.17 (s, 6H), 2.25 (s, 3H), 2.28 (s, 2H), 3.18, 3.37 (s, 2H, AB system, J = 18.80 Hz), 6.36 (s, 1H), 7.08–7.21 (m, 4H), 7.8 (m, 2H), 8.2–8.3 (m, 2H); ^{13}C NMR (125 MHz, CDCl$_3$) δ: 21.6, 28.8, 29.1, 35.0, 38.4, 51.3, 65.1, 118.9, 127.4, 128.0, 128.3, 129.3, 129.5, 129.7, 133.8, 134.8, 138.8, 151.1, 154.6, 156.3, 192.5; %; IR (KBr, cm^{-1}): 2898, 1661, 1652, 1602, 1596, 1491, 1085, 825, 788, 685, 624, 493.

3,4-Dihydro-3,3-dimethyl-13-(4-(methylthio)phenyl)-2H-indazolo[2,1-b]phthalazine-1,6,11(13H)-trione (5o)

Yellow powder, M.P. = 230–232 °C, ^{1}H NMR (500 MHz, CDCl$_3$) δ: 1.21 (s, 6H), 2.34 (s, 2H), 2.42 (s, 3H), 3.21–3.45 (2H, AB system, J = 18.50 Hz), 6.4 (s, 1H), 7.10–7.35 (dd, 4H, J = 8.45 Hz), 7.84–7.88 (2H, m), 8.25–8.37 (m, 2H); ^{13}C NMR (125 MHz, CDCl$_3$) δ: 15.5, 28.4, 28.7, 34.6, 38.0, 50.9, 64.6, 118.3, 126.6 (2C), 127.6 (2C), 127.7, 127.9, 128.9, 129.0, 133.0, 133.5, 134.5, 139.2, 150.9, 154.3, 156.0, 192.1; IR (KBr, cm^{-1}): 2955, 1663, 1629, 1364, 1271, 697; Anal. Calcd for C$_{24}$H$_{22}$N$_2$O$_3$S: C, 68.90; H, 5.30; N, 6.71 %, Found: C, 68.82; H, 5.21; N, 6.78 %.

3,4-Dihydro-3,3-dimethyl-13-(4-isopropylphenyl)-2H-indazolo[2,1-b]phthalazine-1,6,11(13H)-trione (5q)

Yellow powder, M.P. = 229–230 °C, ^{1}H NMR (500 MHz, CDCl$_3$) δ: 1.22–1.25 (m, 12H), 2.37 (s, 2H), 2.9 (m, 1H), 3.26 (d, 1H, AB system, J = 19.05 Hz), 3.42 (d, 1H, AB system, J = 19.05 Hz), 6.47 (s, 1H), 7.19–7.36 (m, 4H), 7.86–7.88 (m, 2H), 8.3–8.4 (m, 2H); ^{13}C NMR (125 MHz, CDCl$_3$) δ: 24.2, 28.5, 29.0, 34.1, 35.3, 35.9, 51.9, 64.8, 111.3, 112.0, 114.6, 118.3, 119.2, 121.4, 123.0, 123.9, 127.2, 127.5, 128.3, 128.4, 132.2, 132.3, 135.5, 136.8, 156.4, 158.8, 191.3.

3,4-Dihydro-3,3-dimethyl-13-(2,3,4-trimethoxy-phenyl)-2H-indazolo[2,1-b]phthalazine-1,6,11(13H)-trione (5r)

Yellow, M.P. = 185–187 °C, ^{1}H NMR (500 MHz, CDCl$_3$) δ: 1.20 (s, 3H), 1.23 (s, 3H), 2.34 (d, 2H, J = 2.60 Hz), 3.26 (d, 1H, AB system, J = 18.60 Hz), 3.42 (d, 1H, AB system, J = 18.60 Hz), 3.83 (s, 3H), 3.84 (s, 3H), 3.86 (s,

3H), 6.58 (s, 1H), 6.67 (d, 1H, J = 9.00 Hz), 7.08 (d, 1H, J = 8.50 Hz), 7.86–7.88 (m, 2H), 8.29–8.31 (m, 1H), 8.38-8.40 (m, 1H); ^{13}C NMR (125 MHz, CDCl$_3$) δ: 28.4, 28.6, 30.9, 34.7, 38.1, 51.0, 55.8, 56.1, 60.6, 60.9, 62.0, 118.3, 127.6, 127.9, 129.0, 129.2, 133.4, 134.4, 142.1, 151.0, 152.0, 154.0, 154.1, 156.1, 157.2, 192.3; IR (KBr, cm^{-1}): 2963, 2651, 1667, 1366, 1287, 1099, 796; Anal. calcd for C$_{26}$H$_{26}$N$_2$O$_6$: C, 67.52; H, 5.67; N, 6.06 %, Found: C, 67.48; H, 5.63; N, 6.09 %.

3,4-Dihydro-3,3-dimethyl-13-(4-propoxy-phenyl)-2H-indazolo[2,1-b]phthalazine-1,6,11(13H)-trione (5s)

Yellow, M.P. = 160–162 °C, ^{1}H NMR (500 MHz, CDCl$_3$) δ: 0.93 (t, 3H, J = 7.00 Hz), 1.23 (s, 3H), 1.25 (s, 3H), 1.73–1.79 (m, 2H), 2.37 (s, 2H), 3.26 (d, 1H, AB system, J = 19.00 Hz), 3.44 (d, 1H, AB system, J = 19.00 Hz), 3.92 (t, 2H, J = 6.50 Hz), 6.44 (s, 1H), 6.86 (d, 2H, J = 8.5 Hz), 7.34 (d, 2H, J = 8.50 Hz), 7.86–7.88 (m, 2H), 8.29–8.30 (m, 1H), 8.36–8.38 (m, 1H); ^{13}C NMR (125 MHz, CDCl$_3$) δ: 14.0, 22.4, 28.2, 28.5, 28.7, 28.9, 34.7, 38.1, 51.0, 64.6, 67.9, 114.6, 118.6, 127.7, 127.9, 128.0, 128.5, 129.0, 129.2, 133.5, 134.5, 150.7, 154.3, 156.1, 159.4, 192.3; IR (KBr, cm^{-1}): 2955, 1669, 1365, 704; Anal. calcd for C$_{26}$H$_{26}$N$_2$O$_4$: C, 72.54; H, 6.09; N, 6.51 %, Found: C, 72.38; H, 5.94; N, 6.66 %.

3,4-Dihydro-3,3-dimethyl-13-(naphthalen-2-yl)-2H-indazolo[2,1-b]phthalazine-1,6,11(13H)-trione (5t)

M.P. = 249-251 ∘C, ^{1}H NMR (500 MHz, CDCl$_3$) δ: 1.16 (s, 6H), 2.27 (s, 2H), 3.22 (d, 1H, J = 19.10 Hz), 3.41 (d, 1H, J = 19.15 Hz), 6.54 (s, 1H), 7.37–7.42 (m, 3H), 7.71–7.90 (m, 6H), 8.16–8.33 (m, 2H); ^{13}C NMR (125 MHz, CDCl$_3$) δ: 28.7, 29.0, 35.0, 38.4, 51.3, 65.4, 118.8, 124.6, 126.6, 126.7, 127.2, 128.0, 128.0, 128.3, 128.6, 129.0, 129.4, 133.5, 133.7, 133.9, 134.1, 134.9, 151.3, 154.7, 156.4, 192.4; IR (KBr, cm^{-1}): 2954, 1665, 1617, 1578, 1470, 1265; Anal. Calcd for C$_{27}$H$_{22}$N$_2$O$_3$: C, 76.76; H, 5.25; N, 6.63 %, Found: C, 76.61; H, 5.17; N, 6.51 %.

3,4-Dihydro-3,3-dimethyl-13-(thiophen-2-yl)-2H-indazolo[2,1-b]phthalazine-1,6,11(13H)-trione (5v)

Yellow powder, M.P. = 219–220 °C, ^{1}H NMR (500 MHz, CDCl$_3$) δ: 1.22 (s, 6H), 2.34 (2H, AB system), 3.25 (1H, AB system, J = 18.5 Hz), 3.46 (1H, AB system, J = 18.00 Hz,), 6.24 (s, 1H), 6.79 (d, 1H, J = 9.00 Hz), 6.98 (t, 1H, J = 9.00 Hz), 7.09 (d, 1H, J = 9.00 Hz), 7.68 (d, 2H, J = 8.25 Hz), 8.04 (d, 2H, J = 8.20 Hz); ^{13}C NMR (125 MHz, CDCl$_3$) δ: 24.4, 28.1, 29.3, 34.4, 35.0, 35.6, 51.9, 64.7, 116.0, 123.5, 125.6, 126.6, 127.0, 127.4, 128.5, 128.9, 132.1, 132.5, 135.7, 139.0, 155.4, 158.6, 191.3; IR

(KBr, cm^{-1}): 2958, 1661, 1575, 1470, 1258; Anal. Calcd for $C_{21}H_{18}N_2O_3S$: C, 66.65; H, 4.79; N, 7.40 %, Found: C, 66.54; H, 4.86; N, 7.31 %.

3,4-Dihydro-3,3-dimethyl-13-(5-bromothiophen-2-yl)-2H-indazolo[2,1-b]phthalazine-1,6,11(13H)-trione (5w)

Yellow, M.P. = 205–207 °C, ^{1}H NMR (500 MHz, CDCl$_3$) δ: 2.29–2.34 (m, 2H), 2.52–2.61 (m, 2H), 3.28–3.35 (m, 1H), 3.56–3.62 (m, 1H), 6.73 (s, 1H), 6.94 (d, 1H, $J = 3.60$ Hz), 7.06 (d, 1H, $J = 4.50$ Hz), 7.86–7.92 (m, 2H), 8.34–8.37 (m, 2H); ^{13}C NMR (125 MHz, CDCl$_3$) δ: 22.3, 24.5, 36.9, 59.5, 113.2, 117.7, 127.8, 128.2, 128.5, 128.8, 128.9, 129.9, 133.8, 134.7, 140.1, 153.4, 154.4, 156.0, 192.4; IR (KBr, cm^{-1}): 3451, 1664, 1363, 1263, 1141, 1109, 1004, 806, 702; Anal. calcd for $C_{19}H_{13}BrN_2O_3S$: C, 53.16; H, 3.05; N, 6.53. Found: C, 52.27; H, 2.95; N, 6.69.

3,4-Dihydro-3,3-dimethyl-13-(1H-indol-3-yl)-2H-indazolo[2,1-b]phthalazine-1,6,11(13H)-trione (5x)

Yellow powder, M.P. = 250–251 °C, ^{1}H NMR (500 MHz, CDCl$_3$) δ: 1.23 (s, 6H), 2.33 (2H, AB system), 3.24 (1H, AB system, $J = 18.50$ Hz,), 3.43 (1H, AB system, $J = 18.00$ Hz), 6.43 (s, 1H), 7.32–8.46 (m, 9H), 9.87 (brs, 1H); ^{13}C NMR (125 MHz, CDCl$_3$) δ: 24.2, 28.5, 29.0, 34.1, 35.3, 35.9, 51.9, 64.8, 111.3, 112.0, 114.6, 118.3, 119.2, 121.4, 123.0, 123.9, 127.2, 127.5, 128.35, 128.39, 132.21, 132.29, 135.5, 136.8, 156.4, 158.8, 191.3; Anal. Calcd for $C_{25}H_{21}N_3O_3$: C, 72.98; H, 5.14; N, 10.21 %, Found: C, 73.08; H, 5.06; N, 10.15 %.

3,4-Dihydro-3,3-dimethyl-13-(ethyl)-2H-indazolo[2,1-b]phthalazine-1,6,11(13H)-trione (5z)

Yellow powder, M.P. = 145–147 °C, ^{1}H NMR (500 MHz, CDCl$_3$) δ: 0.73–0.77 (t, 3H), 1.23 (s, 3H), 1.44 (s, 3H), 2.07–2.17 (m, 1H), 2.39 (m, 2H), 2.39 (s, 2H) 2.51–2.59 (m, 1H), 3.11–3.39 (2H, AB system, $J = 18$ Hz), 5.72–5.73 (m, 1H), 7.83–7.93 (m, 2H), 8.31–8.39 (m, 2H); ^{13}C NMR (125 MHz, CDCl$_3$) δ: 7.2, 22.1, 28.3, 28.8, 34.4, 38.1, 51.0, 63.5, 117.6, 127.5, 127.8, 128.9, 129.0, 133.4, 134.4, 151.8, 155.3, 156.4, 193.0; IR (KBr, cm^{-1}) 2961, 1664, 1622, 1571, 1471, 1421, 1369, 1251; Anal. Calcd for $C_{19}H_{20}N_2O_3$: C, 70.35; H, 6.21; N, 8.64 %, Found: C, 70.23; H, 6.32; N, 8.54 %.

3,4-Dihydro-3,3-dimethyl-13-(hexyl)-2H-indazolo[2,1-b]phthalazine-1,6,11(13H)-trione (5aa)

Yellow powder, M.P. = 84–86 °C, ^{1}H NMR (500 MHz, CDCl$_3$) δ: 0.83–0.85 (t, 3H), 1.12–1.14 (m, 2H), 1.17–1.34 (m, 12H, 3CH$_2$, 2CH$_3$), 2.12–2.13 (m, 1H), 2.44–2.46

(dd, 2H), 2.47–2.50 (m, 1H), 3.15–3.39 (2H, AB system, $J = 19.25$ Hz), 5.73–5.74 (m, 1H), 7.88–7.93 (m, 2H), 8.37–8.41 (m, 2H); ^{13}C NMR (125 MHz, CDCl$_3$) δ: 14.3, 22.9, 23.7, 28.8, 29.2, 29.3, 29.7, 32.0, 34.9, 38.5, 51.4, 63.3, 117.7, 127.9, 128.3, 129.4, 133.8, 134.8, 152.0, 155.0, 156.5, 193.4; IR (KBr, cm^{-1}) 2960, 2927, 1656, 1625, 1574, 1473, 1419, 1362, 1255; Anal. Calcd for $C_{23}H_{28}N_2O_3$: C, 72.60; H, 7.42; N, 7.36 %, Found: C, 72.49; H, 7.52; N, 7.27 %.

References

1. P. Li, S. Regati, R.J. Butcher, H.D. Arman, Z. Chen, S. Xiang, B. Chen, C.G. Zhao, Tetrahedron Lett. **52**, 6220 (2011)
2. B. Willy, T.J. Muller, Eur. J. Org. Chem. **24**, 4157 (2008)
3. V.P. Litvinov, Russ. Chem. Rev. **72**, 69 (2003)
4. Q.R. Zhang, D.Q. Xue, P. He, K.P. Shao, P.J. Chen, Y.F. Gu, J.L. Ren, L.H. Shan, H.M. Liu, Bioorg. Med. Chem. Lett. **24**, 1236 (2014)
5. L. Zhang, L.P. Guan, X.Y. Sun, C.X. Wei, K.Y. Chai, Z.S. Quan, Chem. Bio. Drug Des. **73**, 313 (2009)
6. R. Ghorbani-Vaghei, R. Karimi-Nami, Z. Toghraei-Semiromi, M. Amiri, M. Ghavidel, Tetrahedron **67**, 1930 (2011)
7. G. Shukla, R.K. Verma, G.K. Verma, M.S. Singh, Tetrahedron Lett. **52**, 7195 (2011)
8. M.V. Reddy, G.C.S. Reddy, Y.T. Jeong, Tetrahedron **68**, 6820 (2012)
9. R. Fazaeli, H. Aliyan, N. Fazaeli, Open Cat. J. **3**, 14 (2010)
10. H.R. Shaterian, E. Mollashahi, A. Biabangard, J. Chem. Soc. Pak. **35**, 329 (2013)
11. A. Khalafi-Nezhad, M. Divara, F. Panahi, RSC Adv. **5**, 2223 (2015)
12. B. Karami, V. Ghashghaee, S. Khodabakhshi, Catal. Commun. **20**, 71 (2012)
13. Varsha Brahmkhatri, Anjali Patel, Ind. Eng. Chem. Res. **50**, 13693 (2011)
14. M. Esmaeilpour, J. Javidi, F. Dehghani, F. Nowroozi, Dodeji. New J. Chem. **38**, 5453 (2014)
15. M. Esmaeilpour, J. Javidi, M. Zandi, Mater. Res. Bull. **55**, 78 (2014)
16. A. Khalafi-Nezhad, F. Panahi, R. Yousefi, S. Sarrafi, Y. Ghola-malipour, J. Iran. Chem. Soc. **11**, 1311 (2014)
17. M. Esmaeilpour, J. Javidi, M. Zandi, New J. Chem. **39**, 3388 (2015)
18. J. Javidi, M. Esmaeilpour, Z. Rahiminezhad, F. Nowroozi, Dodeji. J. Clust. Sci. **25**, 1511 (2014)
19. J. Javidi, M. Esmaeilpour, F. Nowroozi Dodeji, RSC Adv. **5**, 308 (2015)
20. D.H.W. Hubert, M. Jung, A.L. German, Adv. Mater. **12**, 1291 (2000)
21. M. Salavati-Niasari, J. Javidi, M. Dadkhah, Comb. Chem. High Throughput Screening **16**, 458 (2013)
22. C.B. Gorman, J.C. Smith, Acc. Chem. Res. **34**, 60 (2001)
23. R. Heerbeek, P.C.J. Kamer, P.W.N.M. Leeuwen, J.N.H. Reek, Chem. Rev. **102**, 3717 (2002)
24. A.J.L. Villaraza, A. Bumb, M.W. Brechbiel, Chem. Rev. **110**, 2921 (2010)

25. M. Salavati-Niasari, J. Javidi, J. Clust. Sci. **23**, 1019 (2012)
26. R.S. Kalhapure, M.K. Kathiravan, K.G. Akamanchi, T. Govender, Pharm. Dev. Technol. **20**, 22 (2015)
27. M. Esmaeilpour, J. Javidi, F. Nowroozi Dodeji, M. Mokhtari Abarghoui, J. Mol. Catal A Chem. **393**, 18 (2014)
28. A.E. Torkamani, P. Juliano, S. Ajlouni, T.K. Singh, Ultrason. Sonochem. **21**, 951 (2014)
29. A. Kumar, R. A. Maurya, Synlett **6**, 883 (2008)
30. M. Esmaeilpour, J. Javidi, F. Nowroozi Dodeji, M. Mokhtari Abarghoui, Transition Met. Chem. **39**, 797 (2014)
31. L.T. Aany Sofia, K. Asha, M. Sankar, N.K. Kala Raj, P. Manikandan, P.R. Rajamohanan, T.G. Ajithkumar, J. Phys. Chem. C **113**, 21114 (2009)
32. A.S. Ertürk, M. Tülü, A.E. Bozdoğan, T. Parali, Eur. Polym. J. **52**, 218 (2014)
33. M. Esmaeilpour, J. Javidi, M. Mokhtari Abarghoui, F. Nowroozi Dodeji, J. Iran Chem. Soc. **11**, 499 (2014)
34. X.-M. Yan, J.-H. Lei, D. Liu, Y.-C. Wu, W. Liu, Mater. Res. Bull. **42**, 1905 (2007)
35. J. Wang, S. Zheng, Y. Shao, J. Liu, Z. Xu, D. Zhu, J. Colloid. Interf. Sci. **349**, 293 (2010)
36. M. Shekouhy, A. Hasaninejad, Ultrason. Sonochem. **19**, 307 (2012)
37. X.N. Zhao, G.F. Hu, M. Tang, T.T. Shi, X.L. Guo, T.T. Li, Z.H. Zhang, RSC Adv. **4**, 51089 (2014)
38. A. Hasaninejed, M.R. Kazerooni, A. Zare, Catal. Today **196**, 148 (2012)
39. G. Sabitha, C. Srinivas, A. Raghavendar, J.S. Yadav, Helv. Chim. Acta **93**, 1375 (2010)
40. H. Veisi, A.A. Manesh, N. Khankhani, R. Ghorbani-Vaghei, RSC Adv. **4**, 25057 (2014)
41. E. Mosaddegh, A. Hassankhani, Tetrahedron Lett. **52**, 488 (2011)
42. H.R. Shaterian, F. Khorami, A. Amirzadeh, R. Doostmohammadi, M. Ghashang, J. Iran. Chem. Res. **2**, 57 (2009)
43. A.R. Kiasat, S. Noorizadeh, M. Ghahremani, S.J. Saghanejad, J. Mol. Struct. **1036**, 216 (2013)
44. L. Nagarapu, R. Bantu, H.B. Mereyala, J. Heterocycl. Chem. **46**, 728 (2009)
45. B. Maleki, S. Sedigh-Ashrafi, R. Tayebee, RSC Adv. **4**, 41521 (2014)
46. J.M. Khurana, D. Magoo, Tetrahedron Lett. **50**, 7300 (2009)
47. X. Wang, W.W. Ma, L.Q. Wu, F.L. Yan, J. Chin. Chem. Soc. **57**, 1341 (2010)